Distributed Jamming Method for ASLC Systems Based on Random Phase Perturbation

Liang Qi * and Jianjiang Zhou

Posted Date: 6 May 2026

doi: 10.20944/preprints202605.0334.v1

Keywords: adaptive sidelobe cancellation; distributed jamming; random phase perturbation; non-stationary jamming; synchronization accuracy

 doi:10.20944/preprints202605.0334.v1

Article

Distributed Jamming Method for ASLC Systems Based on Random Phase Perturbation

Liang Qi [1,2,*] and Jianjiang Zhou [2]

[1] School of Electronic Information Engineering, Nanjing University of Aeronautics and Astronautics, Nanjing 210016, China

[2] No. 723 Institute of China State Shipbuilding Corporation Limited, Yangzhou 225101, China

* Correspondence: ql15380391990@126.com; Tel.: +86-15380391990

Highlights

What are the main findings?

- A distributed jamming method based on random phase perturbation is proposed to disrupt the null tracking capability of ASLC systems. By actively applying random jumps to the relative phase between two spatially separated jamming sources, the equivalent wavefront direction of the combined signal changes rapidly, forming a non-stationary jamming that effectively degrades ASLC performance.
- Monte Carlo simulation results show that the proposed method reduces the average ASLC cancellation ratio from 26.80 dB to 19.73 dB (a decrease of 7.07 dB). The time synchronization error and phase synchronization error have little impact on the jamming effectiveness, demonstrating the robustness of the method to synchronization inaccuracies.

What are the implications of the main findings?

- The proposed method provides an effective and resource-efficient jamming strategy against ASLC systems using only two jamming sources, achieving equivalent direction agility without requiring precise transmission timing control. It offers a theoretical basis and parameter design references for the engineering implementation of distributed cooperative jamming.
- The method exhibits strong robustness to time and phase synchronization errors, making it suitable for practical deployment where synchronization precision is limited. Moreover, the underlying random phase perturbation principle can be extended to other scenarios requiring non-stationary jamming or spatial direction agility.

Abstract

Adaptive Sidelobe Cancellation (ASLC) is a core technology for modern radar systems to suppress active sidelobe jamming. From the perspective of disrupting the ASLC system's ability to stably track the jamming direction, this paper proposes a distributed jamming method based on random phase perturbation. The method employs two spatially separated jamming sources that simultaneously transmit coherent signals. By actively applying controllable random jumps to the relative phase between the two sources, the equivalent wavefront direction of the synthesized signal at the radar receiver changes rapidly, forming a non-stationary jamming that destroys the null-tracking capability of ASLC. An analytical model of the ASLC cancellation ratio under random phase perturbation is established, with a focus on analyzing the effects of time synchronization accuracy and phase synchronization accuracy on jamming performance. Monte Carlo simulation results show that the proposed method can reduce the average ASLC cancellation ratio from 26.80 dB to 19.73 dB (a decrease of 7.07 dB). This study provides a theoretical basis and parameter design references for the engineering implementation of distributed cooperative jamming.

Keywords: adaptive sidelobe cancellation; distributed jamming; random phase perturbation; non-stationary jamming; synchronization accuracy

 doi:10.20944/preprints202605.0334.v1

1. Introduction

Adaptive Sidelobe Cancellation (ASLC) technology is an effective means for modern radar systems to suppress active sidelobe jamming and has been widely deployed in various radar equipment [1,2]. By placing several auxiliary antenna elements around the main antenna, this technology utilizes the high correlation of jamming signals received by the main and auxiliary channels, adaptively adjusts the weights of the auxiliary channels, and forms nulls in the jamming direction, thereby achieving jamming suppression [3,4]. The basic principles and engineering implementation of ASLC are systematically elaborated in [5,6]. However, theoretical analysis indicates that the cancellation performance of ASLC is constrained by multiple factors, resulting in a significant gap between practical cancellation effects and the theoretical limit [7,8]. These factors include channel amplitude-phase inconsistency, delay-bandwidth product, noise, and non-stationary characteristics of jamming signals [9,10,11].

Research on jamming methods against ASLC systems has been mainly carried out by scholars both domestically and internationally in the following directions: first, consuming radar spatial degrees of freedom by increasing the number of jamming sources to achieve multi-directional saturation jamming [12,13]; second, using fast changes in the polarization domain to destroy the polarization consistency between the main and auxiliary channels, implementing cross-polarization or polarization-agile jamming [14,15]; third, adopting asynchronous blinking jamming to cause a mismatch between the training samples and the cancellation period of ASLC, leading to weight mismatch [16,17]; fourth, employing a composite jamming strategy that combines multi-source blinking jamming with polarization jamming [5]. Reference [12] analyzed the jamming principles of multi-directional saturation jamming and asynchronous blinking jamming, and simulation results showed that asynchronous blinking jamming is more effective. Reference [14] proposed an alternating orthogonal polarization jamming method from the polarization domain, which uses the inconsistency of the main and auxiliary antenna polarization characteristics to induce amplitude-phase errors, thereby degrading ASLC cancellation performance. Reference [17] proposed a space-polarization domain combined asynchronous blinking jamming method, which comprehensively employs multi-source jamming, asynchronous blinking jamming, and polarization-agile jamming to disrupt the working conditions of ASLC from multiple dimensions.

The above research has provided a rich theoretical foundation for jamming techniques against ASLC systems. However, existing methods still face certain challenges in engineering implementation: multi-directional saturation jamming requires a large number of jamming sources [18]; the performance of asynchronous blinking jamming is sensitive to the switching rate [16]; and polarization jamming is limited by the polarization characteristics of the radar antenna [14]. Therefore, exploring a novel jamming method that balances jamming effectiveness and engineering feasibility is of significant theoretical value and practical importance. Moreover, the configuration of multi-aircraft cooperative jamming directly affects the detection area of ASLC warning radars [19,20].

From the perspective of disrupting the ASLC system's ability to stably track the jamming direction, this paper proposes a distributed jamming method based on random phase perturbation. The method uses two spatially separated jamming sources to simultaneously transmit coherent signals. By applying actively controllable random jumps to the relative phase between the two jamming sources, the equivalent wavefront direction of the synthesized signal at the radar receiver changes rapidly, forming a non-stationary jamming. Compared with existing methods, the proposed method has the following advantages: (1) it achieves equivalent direction agility with only two jamming sources, requiring low resources; (2) by adopting active random phase perturbation, it does not need precise transmission timing control, making engineering implementation simpler; (3) it quantitatively analyzes the influence of time synchronization accuracy and phase synchronization accuracy on jamming performance, thereby providing parameter design references for engineering implementation.

 doi:10.20944/preprints202605.0334.v1

The remainder of this paper is organized as follows. Section 2 introduces the basic principles and vulnerability analysis of the ASLC system. Section 3 presents the distributed jamming method based on random phase perturbation and establishes its theoretical model. Section 4 validates the effectiveness of the proposed jamming method through simulation experiments and analyzes the influence of synchronization accuracy on jamming performance. Section 5 draws the conclusions.

2. Materials and Methods

This section presents the basic principle of ASLC system for sidelobe suppression processing and analyzes the vulnerabilities existing in its processing procedure.

2.1. ASLC System Principle and Signal Model

As shown in Figure 1, the basic structure of the ASLC system consists of one main channel and multiple auxiliary channels [1,2]. In the figure, $\mathbf{Y}$ represents the output signal of the main channel (the weighted sum of the signals from each antenna), $\mathbf{X}$ represents the received signal vector of the auxiliary channels, $\mathbf{X}=[x_1, x_2, \cdots, x_M]^T$, and $\mathbf{W}$ is the sidelobe cancellation weight vector, $\mathbf{W}=[\omega_1, \omega_2, \cdots, \omega_M]^T$. The output after cancellation is $\mathbf{S}=\mathbf{Y}-\mathbf{W}^H\mathbf{X}$, where H denotes conjugate transpose. The purpose of sidelobe cancellation is to minimize the residual interference in the output signal $\mathbf{S}$.

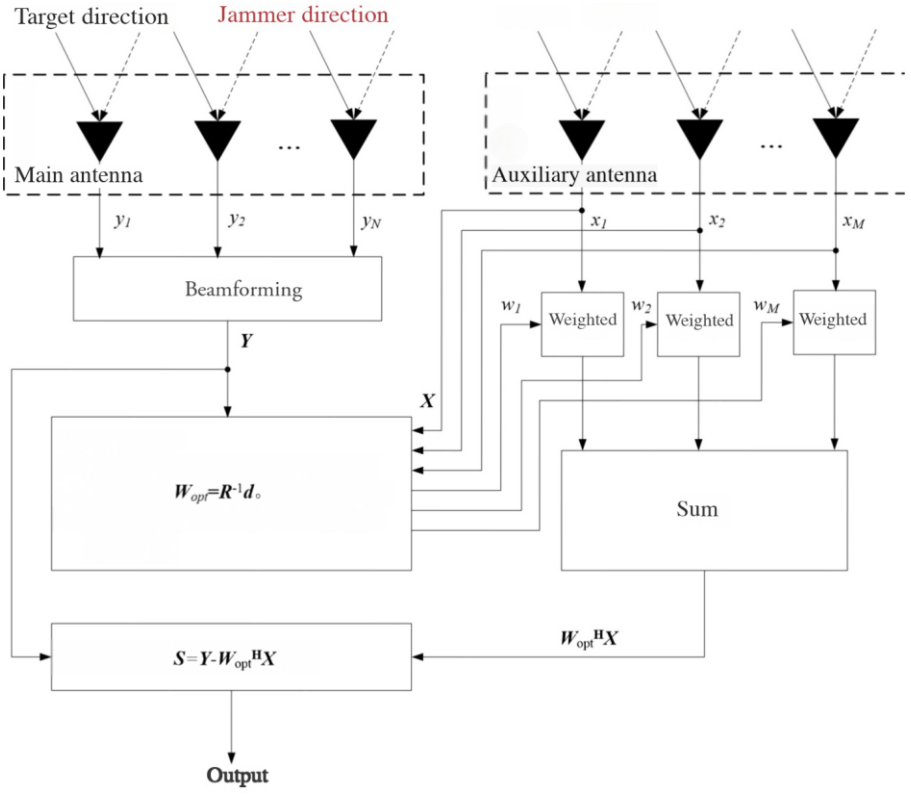

Figure 1. Block diagram of the ASLC system principle.

The optimal weight vector is given by the Wiener-Hopf equation [21]:

$$\mathbf{W}_{opt}=\mathbf{R}_{xx}^{-1}\mathbf{r}_{xy} \quad (1)$$

where $\mathbf{R}_{xx}$ is the covariance matrix of the received signal $\mathbf{X(t)}$ of the auxiliary channels, $\mathbf{R}_{xx}=E(|\mathbf{X}|^2)$, and r_{xy} is the cross-correlation vector between the main channel received signal $\mathbf{Y}(t)$ and the auxiliary channel received signal $\mathbf{X(t)}$, $\mathbf{r}_{xy}=E(\mathbf{XY}^H)$.

For a single strong interference signal $j(t)$ coming from direction θ_j with power $P_j=E\left[|j(t)|^2\right]$, define $\mathbf{g}_{aux}(\theta_j)$ as the M×1 steering vector of the auxiliary channels, $\mathbf{g}_{aux}(\theta_j)=[g_1;g_2;\cdots;g_M]$, where

 doi:10.20944/preprints202605.0334.v1

g_i represents the response of the i-th auxiliary channel to the interference; $G_{main}(\theta_j)$ is the response of the main channel to the interference (a scalar); $\mathbf{n\_aux(t)}$ is the noise vector of the auxiliary channels, $\mathbf{n\_aux(t)}=[n\_aux_1(t);n\_aux_2(t);...;n\_aux_M(t)]$, whose components are independent and identically distributed with covariance matrix $\sigma_{aux}^2\mathbf{I}$; $\mathbf{n\_main(t)}$ is the noise of the main channel (a scalar) with variance σ_{main}^2. Then the received signals of the main and auxiliary channels can be expressed respectively as:

$$\mathbf{X(t)}=\mathbf{g}_{aux}(\theta_j)j(t)+\mathbf{n\_aux(t)} \tag{2}$$

$$\mathbf{Y(t)}=G_{main}(\theta_j)j(t)+\mathbf{n\_main(t)} \tag{3}$$

Further derivation yields the covariance matrix $\mathbf{R}_{xx}$ of the received signal $\mathbf{X}(t)$ of the auxiliary channels:

$$\begin{aligned}\mathbf{R}_{xx}=E[\mathbf{X}(t)\mathbf{X}^H(t)]=E\left[\mathbf{g}_{aux}(\theta_j)|j(t)|^2\mathbf{g}_{aux}^H(\theta_j)\right]+E[\mathbf{g}_{aux}(\theta_j)j(t)\mathbf{n\_aux}^H(t)]+\\ E[\mathbf{n\_aux}(t)j^*(t)\mathbf{g}_{aux}^H(\theta_j)]+E[\mathbf{n\_aux}(t)\mathbf{n\_aux}^H(t)]\end{aligned} \tag{4}$$

Since the interference and noise are uncorrelated, i.e., $E[j(t)\mathbf{n\_aux}^H(t)]=0$ and $E[\mathbf{n\_aux}(t)j^*(t)]=0$, and with $E\left[|j(t)|^2\right]=P_j$ and $E[\mathbf{n\_aux}(t)\mathbf{n\_aux}^H(t)]=\sigma_{aux}^2\mathbf{I}$, we obtain:

$$\mathbf{R}_{xx}=P_j\mathbf{g}_{aux}(\theta_j)\mathbf{g}_{aux}^H(\theta_j)+\sigma_{aux}^2\mathbf{I} \tag{5}$$

Similarly, the cross-correlation vector $\mathbf{r}_{xy}$ between the main and auxiliary channels can be obtained as:

$$\mathbf{r}_{xy}=E[\mathbf{X}(t)\mathbf{Y}^H(t)]=P_j\mathbf{g}_{aux}(\theta_j)G_{main}^*(\theta_j) \tag{6}$$

Substituting equations (5) and (6) into equation (1) and applying the Sherman-Morrison matrix inversion lemma [30], the closed-form expression of $\mathbf{W}_{opt}$ is obtained as:

$$\mathbf{W}_{opt}=\frac{P_jG_{main}^*(\theta_j)}{\sigma_{aux}^2+P_j\|\mathbf{g}_{aux}(\theta_j)\|^2}\mathbf{g}_{aux}(\theta_j) \tag{7}$$

When the interference power is much larger than the noise power, i.e., $P_j\|\mathbf{g}_{aux}(\theta_j)\|^2\gg\sigma_{aux}^2$, the approximate expression of $\mathbf{W}_{opt}$ under high JNR conditions can be obtained as:

$$\mathbf{W}_{opt}\approx\frac{G_{main}^*(\theta_j)}{\|\mathbf{g}_{aux}(\theta_j)\|^2}\mathbf{g}_{aux}(\theta_j) \tag{8}$$

This indicates that the optimal weight vector is completely determined by the spatial steering vector of the interference and is independent of the specific waveform j(t) of the interference. This is precisely the essential reason why ASLC can effectively suppress stationary interference: as long as the interference direction remains unchanged, no matter how the interference waveform varies, ASLC can form a stable null in that direction [11].

In practical radar systems, ASLC usually adopts a segmented processing approach to meet real-time requirements [5]. The system divides the received signal into several time segments. Within each segment, training samples are used to estimate the covariance matrix and the cross-correlation vector, and the optimal weight vector is solved and then applied to the subsequent data of the same segment or to the received signal of the next segment [6]. This segmented processing structure endows ASLC with strong real-time capability and adaptability to interference variations. Studies have shown that properly configuring delay taps in the auxiliary channels can further improve the cancellation performance of ASLC [1].

2.2. Vulnerability Analysis of the ASLC System

 doi:10.20944/preprints202605.0334.v1

The cancellation performance of the ASLC system relies on a core prerequisite: the interference signal is stationary within the covariance matrix estimation window, i.e., its statistical characteristics (power, direction) do not change over time [11]. When this prerequisite is violated, the performance of ASLC degrades significantly [16].

From the signal model, it can be seen that the cancellation effect of ASLC depends on the correlation between the interference signals in the main and auxiliary channels [9]. The correlation coefficient of the interference signals in the main and auxiliary channels is defined as:

$$\varrho=\frac{E[\mathbf{X}(t)Y^{H}(t)]}{\sqrt{E[|\mathbf{X}(t)|^2]E[|\mathbf{Y}(t)|^2]}} \tag{9}$$

Under ideal conditions, $|\varrho|=1$, and ASLC can achieve complete cancellation [7]. However, various factors can cause the correlation coefficient to decrease, including channel amplitude-phase inconsistency [9], channel noise [10], and non-stationary characteristics of the interference [16]. Amplitude-phase errors directly lead to amplitude-phase inconsistency between the main and auxiliary channels, thereby reducing the correlation coefficient and affecting cancellation performance [9,10]. The decorrelation effect of inter-channel noise also reduces the correlation coefficient [10]. When the statistical characteristics of the interference change significantly within the covariance matrix estimation window, the covariance matrix estimation based on finite samples becomes biased, resulting in weight mismatch [16,22].

In response to the above vulnerabilities, various jamming methods have been proposed [12,13]. Multi-directional saturation jamming consumes radar spatial degrees of freedom by increasing the number of jamming sources; when the number of jamming sources exceeds the number of auxiliary channels, the covariance matrix of ASLC becomes rank-deficient, and the weight vector cannot be solved effectively [12]. Asynchronous blinking jamming exploits the timing characteristics of ASLC segmented processing; by rapidly switching the jamming direction, it makes the jamming direction within the training window inconsistent with that within the cancellation window, leading to weight mismatch [16,17]. Polarization jamming takes advantage of the inconsistency between the polarization characteristics of the main and auxiliary antennas, and rapidly changes the polarization state of the jamming signal to destroy the amplitude-phase consistency and correlation between the main and auxiliary channels [14,15,23]. These methods attack the vulnerable links of ASLC from the spatial, temporal, and polarization domains, respectively [5,18].

However, there is a certain contradiction between jamming effectiveness and engineering feasibility in existing methods [24]. Multi-directional saturation jamming requires coordination of multiple jamming sources and consumes significant resources [12,13]. The jamming effectiveness of asynchronous blinking jamming is sensitive to the switching rate, which must be precisely matched to the training window length of ASLC; switching too fast or too slow may lead to a significant degradation of jamming effectiveness, and the parameter setting lacks robustness [16]. Polarization jamming is limited by the polarization characteristics of the radar antenna and lacks universality [14]. Therefore, exploring a novel jamming method that requires low resources, has adjustable synchronization requirements, and provides controllable jamming effectiveness has become an important direction in ASLC countermeasure research [23,25]. Furthermore, the configuration of multi-aircraft cooperative jamming directly affects the detection area of ASLC warning radars [19,20].

3. Distributed Jamming Method Based on Random Phase Perturbation

This section presents the mechanism and system model of the distributed jamming method based on random phase perturbation, discusses the influence of synchronization accuracy on the method in engineering implementation, and finally provides a theoretical analysis of the jamming effectiveness based on the definition of the jamming cancellation ratio.

3.1. Jamming Mechanism and System Model

 doi:10.20944/preprints202605.0334.v1

The core physical mechanism of the proposed distributed jamming method based on random phase perturbation is as follows: by using two spatially separated jamming sources and actively controlling the relative phase between them to jump rapidly and randomly, the equivalent wavefront direction of the synthesized jamming signal received by the radar changes rapidly over time, thereby destroying the null-tracking capability of the ASLC system against jamming from a fixed direction. This is a typical non-stationary jamming strategy.

Assume that two jamming sources are located at spatial angles θ_1 and θ_2, respectively, and transmit the same baseband signal $s(t)$. This baseband signal can be generated by a Direct Digital Synthesizer (DDS) and achieve random jumps through phase perturbation [15]. However, an actively controllable random phase jump $\Delta\Phi_{active}(t)$ is added to the signal of the second jamming source relative to the first one. Then the transmitted signals of the two jamming sources are: $s_1(t)=s(t)$, $s_2(t)=s(t)e^{j\Delta\Phi_{active}(t)}$。When the signals arrive at the radar antenna array, the composite jamming signal received by the main channel is:

$$y_m(t)=G_{main}(\theta_1)s(t)+G_{main}(\theta_2)s(t)e^{j\Delta\Phi_{active}(t)} \tag{10}$$

The equivalent wavefront direction $\theta_{eq}(t)$ of the composite signal is determined by the instantaneous phase difference $\Delta\Phi_{active}(t)$:

$$\theta_{eq}(t)=\frac{1}{2}(\theta_1+\theta_2)+\frac{\Delta\Phi_{active}(t)}{kd\cos(\theta_c)} \tag{11}$$

where $k=2\pi/\lambda$, d is the element spacing, and θ_c is the central angle ($\theta_c \neq \pm 90°$). When $\Delta\Phi_{active}(t)$ jumps rapidly and randomly within $[0, 2\pi)$, $\theta_{eq}(t)$ also varies rapidly, thereby making the jamming exhibit spatial non-stationary characteristics.

The ASLC system estimates the covariance matrix within each training window and assumes that the jamming direction remains constant within that window. When the variation rate of $\theta_{eq}(t)$ exceeds the tracking capability of ASLC, the weight vector estimated within the training window cannot effectively cancel the subsequent jamming, leading to a sharp degradation in cancellation performance.

3.2. Influence of Synchronization Accuracy in Engineering Implementation

In practical engineering, in addition to the actively controllable random jump $\Delta\Phi_{active}(t)$, there also exist additional phase errors introduced by the limitations of time synchronization accuracy and phase synchronization accuracy. Phase noise has a significant limiting effect on the performance of the ASLC system [26,27]. The total phase difference is given by:

$$\Delta\Phi_{total}(t)=\Delta\Phi_{active}(t)+\Delta\Phi_{time}(t)+\Delta\Phi_{phase}(t) \tag{12}$$

where $\Delta\Phi_{time}(t)=2\pi f_c\delta_{time}(t)$ represents the carrier phase shift caused by the time synchronization error $\delta_{time}(t)$ (envelope alignment error), with $\delta_{time}(t)$ obeying a Gaussian distribution with zero mean and standard deviation σ_{time}; $\Delta\Phi_{phase}(t)$ represents the phase synchronization error (residual phase difference of the local oscillators), obeying a Gaussian distribution with zero mean and standard deviation σ_{phase}.

Influence of time synchronization accuracy: The time synchronization error $\delta_{time}(t)$ mainly originates from the initial delay difference between the two jamming sources, clock frequency drift, and propagation path variations. Among these, the initial delay difference introduces a fixed phase offset; clock frequency drift and platform motion cause a slow variation of the phase difference (approximately constant within a single ASLC training window, but drifting between different windows); the fast fluctuation caused by clock random jitter is usually small in magnitude (for high-performance clocks, the phase fluctuation due to random jitter is within about 0.1°). To simplify the analysis, this paper models the overall effect as a zero-mean Gaussian random variable whose standard deviation σ_{time} reflects the time synchronization accuracy. This model encompasses the combined effects of constant bias, slow drift, and random jitter.

 doi:10.20944/preprints202605.0334.v1

Influence of phase synchronization accuracy: The phase synchronization error $\Delta\Phi_{phase}(t)$ mainly originates from the residual phase difference and frequency drift between the local oscillators of the two jamming sources. It typically exhibits slow variation (approximately constant within a single ASLC training window but varying randomly between different windows). To simplify the analysis, this paper models it as a zero-mean Gaussian random variable whose standard deviation σ_{phase} reflects the phase synchronization accuracy. This model not only captures the slow-varying nature of the actual synchronization error but also facilitates Monte Carlo simulation analysis.

Influence of reference clock phase noise: The phase noise of the reference clock itself will generate phase jitter at the radar carrier frequency after frequency multiplication. When a high-performance oven-controlled crystal oscillator (OCXO) is used, the phase noise of the 100 MHz reference clock at a 1 kHz offset can reach –145 dBc/Hz. After multiplication by a factor of 100 to 10 GHz, the phase noise deteriorates by 40 dB, and the equivalent phase jitter is about 0.08°–0.5°. This magnitude is far smaller than the time synchronization error (nanoseconds correspond to tens of degrees) and the active phase jump (0–360°), and thus its impact on the proposed jamming method can be neglected. Therefore, the influence of reference clock phase noise is ignored in the subsequent simulations.

3.3. Theoretical Analysis of Jamming Effectiveness

To quantitatively describe the jamming effectiveness, the ASLC jamming Cancellation Ratio (CR) is defined as:

$$CR=10\log_{10}\left(\frac{P_{before}}{P_{after}}\right) \tag{13}$$

where P_{before} and P_{after} are the interference powers before and after cancellation, respectively [10]. A larger CR indicates better suppression of the interference by ASLC; conversely, a smaller CR indicates more significant jamming effectiveness.

According to adaptive filtering theory, the CR and the correlation coefficient ϱ between the interference signals of the main and auxiliary channels satisfy the following theoretical relationship:

$$CR=10\log_{10}\left(\frac{1}{1-|\varrho|^2}\right) \tag{14}$$

The above equation indicates that when the interference signals of the main and auxiliary channels are perfectly coherent ($|\rho|\to1$), the CR tends to infinity, and ASLC can achieve ideal cancellation. When the correlation decreases ($|\rho|<1$), the CR decreases accordingly. In this paper, Monte Carlo simulations are used to directly compute the CR by statistically evaluating P_{before} and P_{after}, while ϱ is also recorded simultaneously to verify the theoretical relationship between the two.

On this basis, the quantitative relationship between the time synchronization error σ_{time}, the phase synchronization error σ_{phase}, and the CR is further established to provide a basis for engineering parameter design.

4. Simulation Analysis

4.1. Simulation Parameter Setting

To verify the effectiveness of the proposed jamming method, this paper establishes an ASLC system simulation model based on the MATLAB platform. The system parameters are set as follows:

- Radar operating frequency: 10 GHz, element spacing: half wavelength;
- Transmitted signal: linear frequency modulation (LFM) signal, pulse width 10 μs, bandwidth 10 MHz;
- Sampling frequency: 40 MHz, pulse repetition interval: 1 ms;
- Number of main array elements: 32, number of auxiliary channels: 4;
- Target direction: 0°, target range: 100 km, signal-to-noise ratio (SNR): -15 dB;

 doi:10.20944/preprints202605.0334.v1

- Jamming directions: 16° and 25°, jamming-to-noise ratio (JNR): 40 dB;
- ASLC processing: segment length 1000 samples, training window length 64 samples;
- Active random phase jump: jumps every 50 samples, jump values uniformly distributed in [0, 2π);
- Time synchronization error σ_time: scan range 0.1~10 ns;
- Phase synchronization error σ_phase: scan range 1°~30°;

The simulation adopts the Monte Carlo method with 100 Monte Carlo runs, and the average cancellation ratio and its standard deviation are statistically computed.

4.2. Verification of Jamming Effectiveness of Active Random Phase Jumps

To verify the effectiveness of active random phase jumps (without additional synchronization errors), $\sigma_{\text{time}} = 0$ and $\sigma_{\text{phase}} = 0$ are fixed. The two cases of no phase jump ($\Delta\Phi_c(t) = 0$) and phase jump ($\Delta\Phi_c(t)$ jumping randomly every 50 samples) are compared. The results of the last Monte Carlo simulation are shown in Figures 2 and 3.

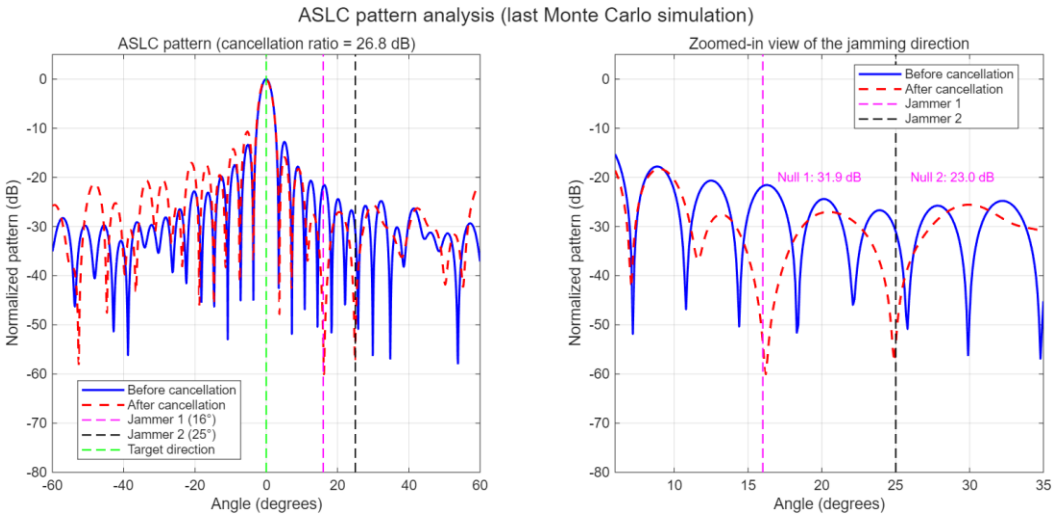

Figure 2. ASLC pattern without phase jump.

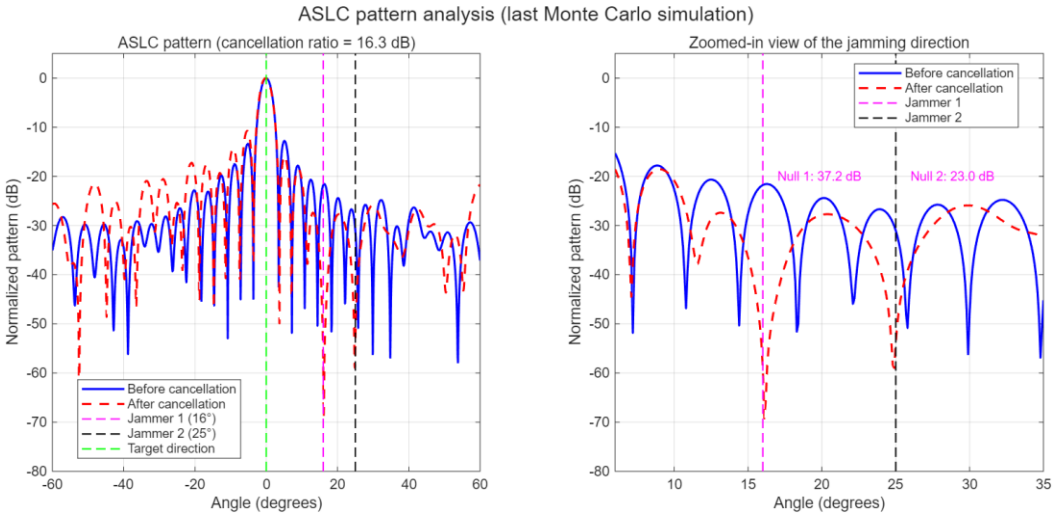

Figure 3. ASLC pattern with phase jump.

As can be seen from Figure 2, in the last Monte Carlo simulation without phase jumps, ASLC cancellation processing can form effective nulls in both jamming directions, with a cancellation ratio of 26.8 dB, achieving good jamming suppression. As can be seen from Figure 3, with phase jumps, although nulls can still be formed in both jamming directions, the null depth in the first jamming

 doi:10.20944/preprints202605.0334.v1

direction (16°) becomes significantly shallower, and the cancellation ratio is only 16.3 dB. This indicates that the phase-jump processing can effectively reduce the jamming suppression capability of ASLC, with the jamming cancellation ratio decreasing by 10.5 dB, thereby verifying the destructive effect of fast equivalent direction changes from two jamming sources on ASLC.

The results of a single simulation have some randomness, and the mean values better represent the overall performance. The statistical results of the Monte Carlo simulations are given in the following table. The statistical means differ slightly from the single-simulation results, but the trends are consistent.

Table 1. Effect of active random phase jumps on ASLC cancellation performance

Condition	Mean cancellation ratio (dB)	Standard deviation of cancellation ratio (dB)	Mean correlation coefficient
No phase jump	26.80	0.03	0.9987
Active random jump (every 50 samples)	19.73	1.22	0.9923

The statistical results show that under the above simulation conditions, compared with the case without phase jumps, the active random phase jump jamming method can reduce the average ASLC cancellation ratio from 26.80 dB to 19.73 dB, a decrease of 7.07 dB. The fundamental reason is that the active random phase jumps reduce the correlation between the main and auxiliary channels, with the correlation coefficient decreasing from 0.9987 to 0.9923, thereby causing a significant degradation in the cancellation performance of ASLC.

4.3. Influence of Time Synchronization Accuracy on Jamming Effectiveness

The active jump parameters are fixed (jump every 50 samples), and the phase synchronization error is set to σ_{phase} =5°. The standard deviation of the time synchronization error σ_{time} is scanned from 0.1 ns to 10 ns. The simulation results are shown in Table 2.

Table 2. Cancellation ratio under different time synchronization errors

σ_{time}(ns)	Mean cancellation ratio(dB)	Standard deviation of cancellation ratio (dB)	Mean correlation coefficient
0.1	19.83	1.24	0.9927
0.5	19.73	1.22	0.9923
1.0	19.75	1.21	0.9925
2.0	19.94	1.22	0.9926
5.0	19.77	1.21	0.9924
10.0	19.84	1.14	0.9927

As can be seen from Table 2, the time synchronization accuracy has little effect on the proposed method, and the cancellation ratio is basically stable in the range of 19.73 dB to 19.94 dB. This is because the phase variation introduced by the time synchronization error can be regarded as a constant value within the ASLC cancellation processing period (1000 samples), while the main factor that destroys the correlation is the fast equivalent direction change caused by the active random phase jumps. When σ_{time} varies from 0.1 ns to 10 ns, the standard deviation of the cancellation ratio does not exceed 1.24 dB, and the mean fluctuation is less than 0.2 dB, indicating that the proposed method is insensitive to time synchronization errors and verifying its robustness to time synchronization accuracy.

4.4. Influence of Phase Synchronization Accuracy on Jamming Effectiveness

 doi:10.20944/preprints202605.0334.v1

The active jump parameters are fixed, the time synchronization error is set to σ_{time}= 0.5 ns, and the standard deviation of the phase synchronization error σ_{phase} is scanned from 1° to 30°. The simulation results are shown in Table 3.

Table 3 Cancellation ratio under different phase synchronization errors

σ_{phase}(°)	Mean cancellation ratio(dB)	Standard deviation of cancellation ratio (dB)	Mean correlation coefficient
1	19.74	1.22	0.9923
5	19.73	1.22	0.9923
10	19.71	1.22	0.9922
15	19.70	1.23	0.9922
20	19.69	1.23	0.9922
30	19.68	1.23	0.9922

As can be seen from Table 3, as the phase synchronization accuracy decreases, the mean cancellation ratio gradually decreases from 19.74 dB to 19.68 dB, indicating a slight enhancement of the jamming effectiveness. This is because, although the phase synchronization error can be considered a constant value within the ASLC cancellation processing period (1000 samples), unlike the phase error introduced by time synchronization accuracy (0.1 ns corresponds to one signal period, i.e., 360°), the randomness of the phase synchronization error (1°–30°) can accumulate over multiple Monte Carlo simulations, making a positive contribution to destroying the correlation between the main and auxiliary channels. This simulation verifies the robustness of the proposed active random phase jump jamming method to phase synchronization accuracy.

5. Conclusions

This paper has proposed a distributed jamming method based on active random phase perturbation to counter the ASLC system. Through theoretical analysis and Monte Carlo simulations, the following conclusions are drawn:

(1) Active random phase jumps cause the equivalent wavefront direction of the combined jamming signal to change rapidly, forming a non-stationary jamming that can effectively destroy the null-tracking capability of ASLC against jamming from a fixed direction. When the jump rate is sufficiently fast, Monte Carlo simulation results show that the average cancellation ratio decreases from 26.80 dB to 19.73 dB.

(2) Within the ASLC processing period (1000 samples), the phases introduced by time synchronization errors and phase synchronization errors can be approximated as constant values, which do not affect the destructive effect of active random jumps on the rapid change of the equivalent direction. Therefore, the proposed method exhibits good robustness to both time synchronization accuracy and phase synchronization accuracy.

(3) The proposed method requires only two jamming sources to achieve equivalent direction agility, striking a good balance among resource requirement, synchronization demand, and jamming effectiveness. It provides a theoretical basis and parameter design references for the engineering implementation of distributed cooperative jamming.

Future research will further consider: (a) optimization strategies for random phase perturbation in multi-source jamming scenarios [28]; (b) adaptive adjustment of perturbation parameters to counter radar anti-jamming countermeasures [29]; (c) combining random phase perturbation with

 doi:10.20944/preprints202605.0334.v1

spatial-domain and polarization-domain jamming techniques to achieve multi-dimensional composite jamming [14,17].

Author Contributions: Conceptualization, L.Q.; Methodology, L.Q.; Validation, L.Q.; Resources, L.Q.; Data curation, L.Q.; Writing—original draft, L.Q.; Writing—review & editing, J.Z. All authors have read and agreed to the published version of the manuscript.

Funding: This research received no external funding.

Institutional Review Board Statement: Not applicable.

Informed Consent Statement: Not applicable.

Data Availability Statement: Data are contained within the article.

Conflicts of Interest: Author Liang Qi was employed by the company No. 723 Institute of China State Shipbuilding Corporation Limited. The remaining authors declare that the research was conducted in the absence of any commercial or financial relationships that could be construed as a potential conflict of interest.

References

1. Yu X.; Su T.; Wu K. ASLC Algorithm and Implementation of Software Radar[J]. Radar Science and Technology, **2017**, 15(3): 285-290.
2. Zhang J.; Song W.; Zhang Z.; Hu M. Performance Analysis and Simulation of Adaptive Sidelobe Cancellation[J]. Radar Science and Technology, **2008**, 6(6): 486-491.
3. Hu K.; Hu A. Application of Adaptive Side-lobe Cancellation in Radar[J]. Fire Control Radar Technology, **2006**, 35(2): 42-45.
4. Zhu J.; Tao L.; Gao X.; Wan X. Principle and Realization of Adaptive Side-lobe Canceling Based on FPGA[J]. Radar Science and Technology, **2003**, 1(3): 183-187.
5. Tan Y.; Tian Y.; Liu M. Study on Adaptive Side-lobe Cancellation about Phased-array Radar[J]. Science Technology and Engineering, **2009**, 9(22): 6829-6831.
6. Zhao N.; Han G.; Zhang J. An Improved Algorithm of Digital Beam Anti-jamming Based on Adaptive Side-lobe Cancellation[J]. Modern Radar, **2024**, 46(6): 74-78.
7. Tang X.; Li R.; Dai L.; Chen F.; Duan K. The Combination of Adaptive Side-lobe Canceler and Moving Target Detection[J]. Radar Science and Technology, **2016**, 14(3): 273-278.
8. Mohammed J.; Sayidmarie K. Performance evaluation of the adaptive side-lobe canceler system with various auxiliary configurations[J]. International Journal of Electronics and Communications, **2017**, 89: 179-185.
9. Jiang J.; Li X.; Ren W. Performance Analysis of ASLC with Amplitude and Phase Error[J]. Electronics Optics & Control, **2009**, 16(5): 52-54.
10. Peng X.; Li R.; Wang Y.; Chen F. Two Methods of Modified Adaptive Channel Equalization[J]. Journal of Electronics & Information Technology, **2006**, 28(4): 658-662.
11. Li X.; Zhang Y. Analysis of ASLC Performance under Wide-band Jamming[J]. Modern Radar, **2008**, 30(3): 34-36.
12. Long S.; Peng S.; Wang Z.; Tang H. Analysis and Comparison of Interference Methods Against the Adaptive Side-lobe Canceling System[J]. Electronic Information Warfare Technology, **2016**, 31(1): 38-42, 60.
13. Li S. Research into The Cooperative Jamming Technology Based on Space Distribution[J]. Shipboard Electronic Countermeasure, **2019**, 42(6): 5-8, 34.
14. Tao J.; Li X.; Huang X. Performance Analysis of ASLC System When Taking Antenna Polarization into Consideration[J]. Journal of Air Force Engineering University (Natural Science Edition), **2010**, 11(2): 38-41.
15. Wang F.; Li C.; Yang X. A New Method for Repressing DDS Spur Based on Second-Order Phase Dithering[J]. Application of Electronic Technique, **2011**, 24(7): 6-9.
16. Li S.; Li Y.; Zhang G.; Guo Y. A Study on Twinkle Jamming Project Against on the Adaptive Sidelobe Canceling System[J]. Modern Radar, **2012**, 34(2): 51-54.

 doi:10.20944/preprints202605.0334.v1

17. Zhang Y.; Pang B.; Dai D.; Chen B. A Joint Spatial-Polarization Domain Asynchronous Blinking Jamming Method Against Radar Sidelobe[J]. Radar Science and Technology, **2025**, 23(6): 1-10.
18. Long S.; Peng S.; Wang Z.; et al. Research into the Configuration of Multi-jammer Cooperative Jamming to Phased Array Radar[J]. Shipboard Electronic Countermeasure, **2015**, 38(6): 1-3.
19. Wang J. Self-defense/Cooperative Jamming against Pulse Doppler Radar[J]. Shipboard Electronic Countermeasure, **2012**, 35(3): 18-22.
20. Duan X.; Fu X.; Gao X. Computation of Detection Coverage for ASLC Warning Radar under Stand-off Jamming[J]. Fire Control & Command Control, **2013**, 38(3): 65-68.
21. Wang X.; Zhai W.; Farina A. A unified framework of adaptive sidelobe canceller design by antenna/subarray selection[J]. Signal Processing, **2021**, 189: 108243.
22. Li X.; Yang S. A Study on the Attack Technology on ASLC in Time Domain[J]. Modern Radar, **2013**, 35(10): 18-21, 26.
23. Wang X. Jamming Mechanism of Variable Polarization Jamming on Radar Side-lobe Cancellation[J]. Modern Defence Technology, **2024**, 52(2): 145-150.
24. Xing M.; Xiao J. Research on Cooperative Jamming in Complex Electromagnetic Environment[J]. Telemetry & Telecontrol, **2010**, 31(4): 30-35.
25. Qi L.; Ma X.; Deng X. Jamming Method of ASLC System Based on Leading Smart Noise[J]. Modern Radar, **2021**, 43(9): 93-98.
26. Wang Q.; Luo K.; Qin H. Impact of Phase Noise on Sidelobe Cancellation System Utilizing Distributed Phase-Lock-Loops[J]. Progress In Electromagnetics Research M, **2023**, 120: 1-14.
27. Zhou M.; Wang Q.; He F.; Zhang Y.; Luo K.; Meng J. Impacts of phase noise on the performance of adaptive side-lobe cancellation system[C]. 2021 IEEE 4th International Conference on Electronic Information and Communication Technology (ICEICT), Xi'an, China, **2021**: 106-109.
28. Pu W.; Feng K.; Wang X.; et al. Enhanced Mainlobe Jamming Suppression in Distributed Array Radar via Joint Optimization of Radar Positions and Subpulse Frequencies[J]. Remote Sensing, **2025**, 17(14): 2423.
29. Liu Q.; Pu W.; Liu H.; Liang Z.; Tian D.; Chen X. Multi-jamming suppression based on iterative reconstruction of jamming spectrum in distributed array radar[J]. Signal Processing, **2026**, 238: 110178.
30. Sherman J.; Morrison W. Adjustment of an inverse matrix corresponding to a change in one element of a given matrix[J]. The Annals of Mathematical Statistics, **1950**, 21(1): 124-127.